Adjusting 3-Pulse Canceller to Enhance Slow Radar Targets

Itzik Cohen, and Nadav Levanon

Dept. of Electrical Engineering – Systems, Tel Aviv University, Tel Aviv, 6997801, Israel

Abstract **Doppler processing of a coherent periodic waveform usually employs an n-pulse (or n-period) canceller followed by a weighted FFT. Early moving target detection (MTD) used a simple 3-pulse canceller as the MTI filter. MTD in ground-based radar faces a conflict between clutter attenuation and slow targets' visibility. The paper suggests two simple modifications to a 3-pulse canceller that will ease this conflict. Detecting very slow targets within stationary clutter gains importance in border or perimeter safeguarding.**

Index Terms **— Radar, Doppler processor, MTI, MTD, pulse-canceller, weight window, clutter attenuation.**

I. Introduction

Early design of MTD (moving target detection) [1, 2, 3] involved a coherent pulse train signal, processed coherently on receive by a 3-pulse canceller, followed by a weighted FFT. The 3-pulse canceller (Fig. 1) is a simple FIR linear filter which results in significant attenuation of clutter return.

The parameters were usually designed with two assumptions: (a) the clutter spectral density is zero-mean Gaussian with standard deviation of σ_ω rad/s; (b) the target's Doppler shift is uniformly distributed between $-1/(2T_r) \le f_D \le 1/(2T_r)$, where T_r is the pulse repetition interval (PRI), or, in case of a periodic continuous waveform (CW), the waveform's period. The design of the 3-pulse canceller originated from cascading two 2-pulse cancellers, which led to binomial weights, namely

$$W_1 = 1,\ W_2 = -2,\ W_3 = 1. \qquad (1)$$

The resulted angular frequency response is

$$\left|H(\omega)\right|^2 = \left|\frac{Y(\omega)}{X(\omega)}\right|^2 = 4\sin^2\left(\frac{\omega T_r}{2}\right). \qquad (2)$$

The response in (2) exhibits nulls at Doppler frequencies $f_D = \pm n/T_r$, $n = 0,1,2,\ldots$, which result in blind velocities.

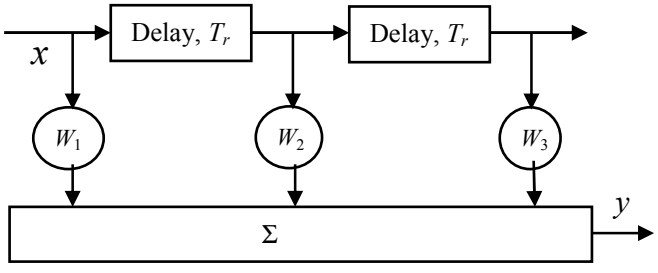

Fig. 1. Estimated Three-pulse canceller.

With assumption (b) and the weights in (1), the improvement in the signal-to-clutter ratio between the input and the output of the 3-pulse canceller is given by namely

$$I = \mathrm{E}\left[\frac{(S/C)_{\text{out}}}{(S/C)_{\text{in}}}\right] = \left[1 - \frac{4}{3}e^{-\frac{1}{2}(\sigma_\omega T_r)^2} + \frac{1}{3}e^{-\frac{1}{2}(2\sigma_\omega T_r)^2}\right]^{-1}. \qquad (3)$$

Optimizing the improvement factor [4, 5] will yield dependence of the middle weight W_2 as function of $\sigma_\omega T_r$ that will differ slightly from –2. Other modifications to the block diagram of the pulse cancelers were suggested very early [6, 7].

The interest in this paper is in very slow targets, so assumption (b) does not hold, and the question is how to significantly attenuate almost stationary clutter and yet do not attenuate slow targets too much. The following sections will discuss two simple modifications to the 3-pulse canceller and then show the expected spectral response of the processor which cascades the modified MTI filter and the FFT-based Doppler processor.

II. 3-Pulse Canceller with Modified Weights

The 3-pulse canceller is used mostly because its frequency response's null is wider than the null of the very simple 2-pulse canceller, and because it is much simpler than IIR filters that can better control the shape of that null [2, 7]. However, when considering a very slow target the added attenuation by the 3-pulse canceller may be too high. The proposed modification provides smooth transition from 2-pulse canceller to 3-pulse canceller. It does so by modifying the three weights in (1) to the weights:

$$W_1 = 1,\ W_2 = -(b+a),\ W_3 = ba. \qquad (4)$$

When $a = 0$, $b = 1$ the filter becomes a 2-pulse canceller, while $a = 1$, $b = 1$ will result in a conventional 3-pulse canceller. A half-way response is obtained at approximately $a = 0.8$, $b = 1$. That response is shown in Fig. 2, next to the responses of the 2 and 3-pulse cancellers. A Gaussian clutter spectrum with $\sigma_\omega T_r = 0.002$ is also shown.

The main result of reducing the parameter a (from 1 to 0.8), while keeping $b = 1$, is to reduce the attenuation at small Doppler velocities. Note in Fig. 2 that while at $f T_r = 0.02$ the attenuation of the 3-pulse canceller decreased by 6.2dB (from 48.1 to 41.9), at $f T_r = 0.002$ the attenuation decreased by 25dB (from 88.1 to 63.1). This boost in the visibility of slow targets is significant but may not be enough in some cases.

978-1-4799-7473-3/15/$31.00 ©2015 IEEE
From *IEEE International Conference on Microwaves, Communications, Antennas and Electronic Systems* (COMCAS 2015), 2 - 4 November 2015, Tel Aviv, Israel

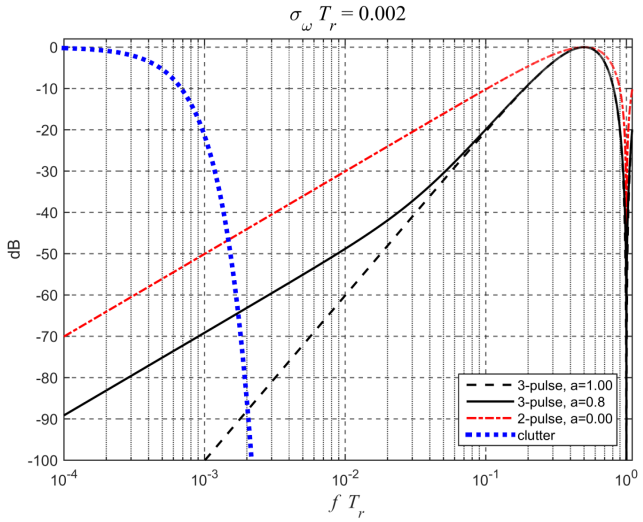

Fig. 2. Frequency response of a modified (eq. 4) 3-pulse canceller (a = 0, 0.8, 1; b = 1).

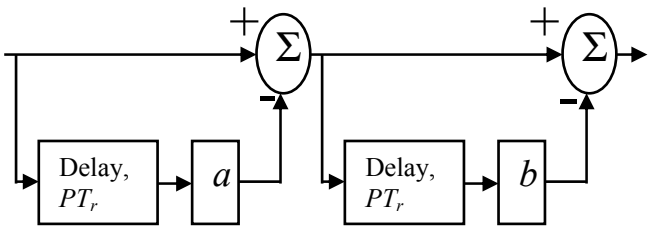

Fig. 3. Modified 3-pulse canceller.

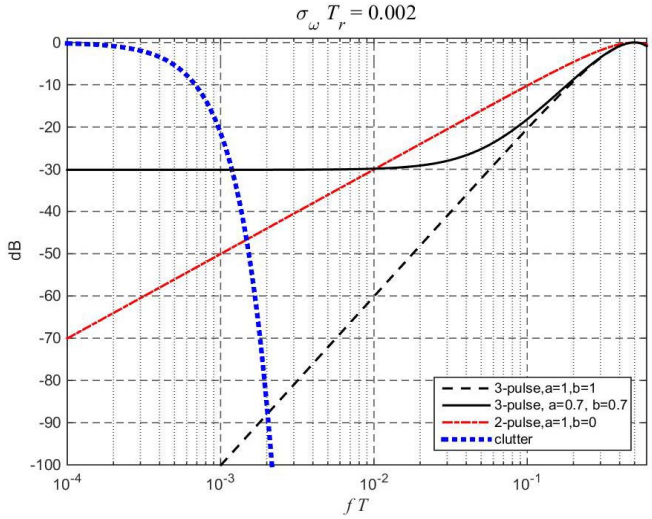

Fig. 4. Frequency response of a modified (eq. 4) 3-pulse canceller (a = 0.7, b = 0.7).

TABLE I
CONVERSION FROM $f T_r$ TO v[m/s], (f_c=9GHz, T_r=25.6μs).

$f T_r$	10^{-4}	10^{-3}	10^{-2}	10^{-1}	1
v [m/s]	0.065	0.65	6.5	65	650

The weight design in (4) corresponds to the block diagram in Fig. 3. Choosing a<1 and b<1 removes the complete null at zero Doppler frequency, which may help raise the response at very low Doppler frequencies (Fig. 4).

III. 3-PULSE CANCELLER WITH MODIFIED DELAYS

When the coherent processing interval (CPI) contains many pulses (or periods) it is possible to increase the delays in Figs. 1 and 3 from a single PRI to several PRIs. The obvious result of increasing the delay from T_r to PT_r (where P is an integer) will be lowering the first blind Doppler by a factor of P. This is acceptable when we are interested in slow targets. The effect at lower Doppler frequencies is demonstrated in Fig. 5 (for P = 16). The general transition from the dimensionless $f_D T_r$ to target radial velocity v in m/s is given in (5) and is listed in Table 1 for few specific values.

$$v = \frac{\mathrm{C}}{2 f_c T_r} f_D T_r = 651 f_D T_r\,,\ f_c = 9\mathrm{GHz}, T_r = 25.6\mu\mathrm{s}\,. \quad (5)$$

In Fig. 5, at $f T_r = 0.002$, (v = 1.3m/s), where slow targets can be found, the attenuation is only 27.8dB. In a conventional 3-pulse canceller (a=1, b=1, P=1) the attenuation, according to Fig. 4, is 88dB. The penalty is the attenuation at $f T_r = 0.0002$, or v = 0.13m/s, where mostly clutter is expected. In a conventional 3-pulse canceller the attenuation is > 100dB, while in the modified canceller it is only 30dB.

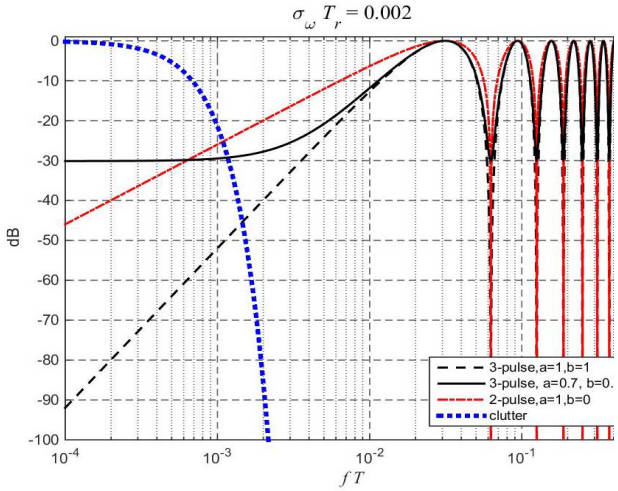

Fig. 5. Frequency response of a modified 3-pulse canceller (a = 0.7, b = 0.7, P = 16).

IV. GENERALIZED IMPROVEMENT FACTOR

The improvement factor I in (3) can be generalized for the new parameters a, b and P. We first update assumption (b) as follows: (b) the target's Doppler shift is uniformly distributed between $-1/(2PT_r) \le f_D \le 1/(2PT_r)$, where PT_r is the delay-line duration. In that case. The more general improvement factor is given in (6). Note that (6) reduces to (3) when $a = 1,\ b = 1, P = 1$.

$$I = \left[1 - \frac{2(a+b)\left(1+a^2b^2\right)}{1+(a+b)^2+a^2b^2} e^{-\frac{1}{2}(\sigma_\omega PT_r)^2} + \frac{2ab}{1+(a+b)^2+a^2b^2} e^{-\frac{1}{2}(2\sigma_\omega PT_r)^2} \right]^{-1} \quad (6)$$

An example of the new 2-dimensional expression of I as function of a and b is shown in Fig. 6, for clutter having zero-mean Gaussian spectrum with $\sigma_\omega P\,T_r = 0.002$. Fig. 6 demonstrates how fast the improvement factor drops as a and/or b are lowered below their nominal value of 1.

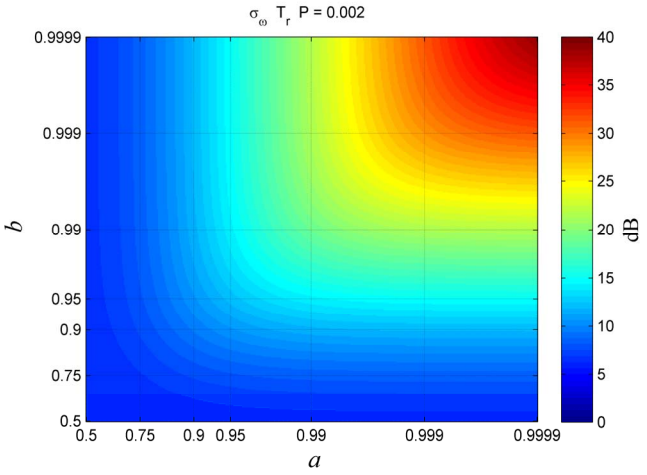

Fig. 6. Improvement factor as function of a and b. Gaussian clutter spectrum with $\sigma_\omega P\,T_r = 0.002$.

Reducing the improvement factor is tolerable because the MTI's response does not describe the entire response. The next step is creating many Doppler filters through the use of weighted FFT. Each filter will have its own response and that response will be multiplied by the response of the modified 3-pulse canceller to yield the final response of each particular Doppler filter.

V. Combined Response of a 3-Pulse Canceller Followed by Weighted FFT Doppler Filter

An important factor in the design of FFT-based Doppler processor is the weighting function. A weighting function [6, 7] lowers the frequency response sidelobes at the cost of widening the mainlobe. The widened mainlobe, or the sidelobes of a low-Doppler window if not lowered enough, my overlap clutter, unless the clutter was sufficiently attenuated by the MTI filter.

The expected frequency responses of MTD with a large (=2048) number of pulses or periods are shown in Figs. 7 (conventional 3-pulse canceller, a=1, b=1, P=1) and 8 (modified 3-pulse canceller, a=0.7, b=0.7, P=16). The major conclusion can be deduced by comparing the bottom subplots of the two drawings. They show the response of

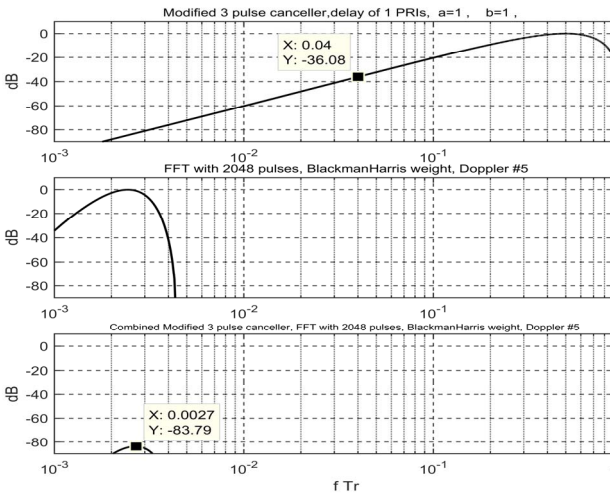

Fig. 7. Frequency response of a conventional 3-pulse canceller (a=1, b=1, P=1), followed by a BlackmanHarris weighted 2048-pulse FFT (Doppler window #5)

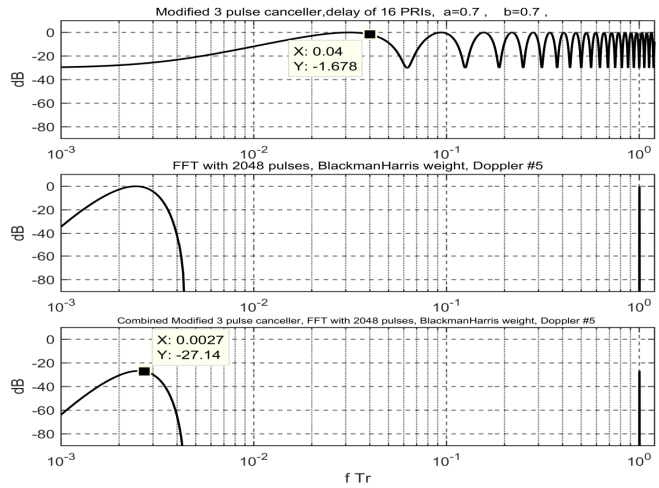

Fig. 8. Frequency response of a modified 3-pulse canceller (a=0.7, b=0.7, P=16), followed by a BlackmanHarris weighted 2048-pulse FFT (Doppler window #5)

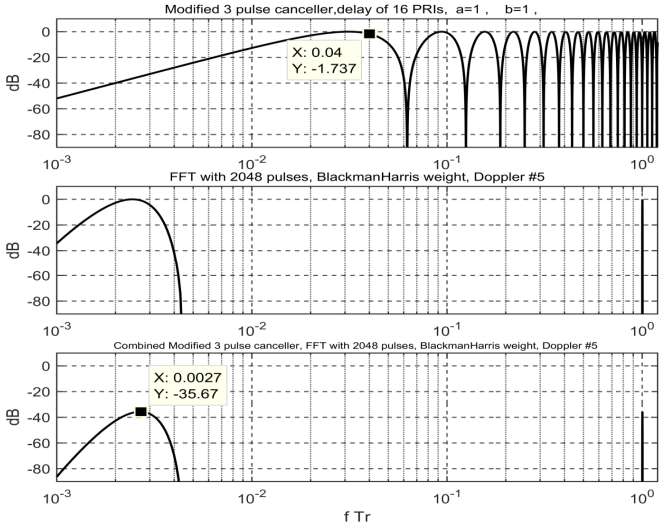

Fig. 9. Frequency response of a conventional 3-pulse canceller (a=1, b=1, P=16), followed by a BlackmanHarris weighted 2048-pulse FFT (Doppler window #5)

the 5th Doppler window centered at $f_D T_r = 0.0027$, $v = 1.63\text{m/s}$. With the conventional 3-pulse canceller (Fig. 7) the 5th Doppler window suffers 84dB attenuation. With the modified canceller (Fig. 8), the attenuation is only 27dB.

Another observation comes from the middle subplots. They show that the 5th FFT window alone attenuates clutter at $f_D T_r = 0.001$, ($v = 0.65\text{m/s}$), by only 34dB. When combined with the modified 3-pulse canceller (Fig. 8) the attenuation increases to 64dB. Additional interesting comparison is seen at $f_D T_r = 0.04$, ($v = 26\text{m/s}$). In Fig. 7 (top subplot) the attenuation of the conventional 3-pulse canceller is 36dB, while in Fig. 8 (top subplot) the attenuation is only 1.7dB. Fig. 9 was added in order to show the disadvantage of the classical binomial parameters (a=1, b=1), compared to the modified parameters (a=0.7, b=0.7). Note that the attenuation at the peak of the 5th Doppler window in Fig. 9 (bottom subplot) increased by 8.5dB when the binomial parameters (a=1, b=1) are used. The practical meaning of those 8.5dB will be demonstrated in the next section.

VI. Experimental Results

The modified 3-pulse canceller was tested with low-power CW phase-coded radar, observing receding cars in a one-way alley from the roof-top of a 4-story building. The radar range resolution is 3.75m and its range-rate resolution is 0.32m/s. The azimuth resolution was rather wide $\left(\approx 30^0\right)$ thus the beam span included buildings, huts and a dirt lot in which an excavator tractor was working (Fig. 10) to which we will refer as "target 1". The delay-Doppler displays of two time-spaced scenes, 1.8s apart, are shown in Figs. 11 when the parameters are (a=0.7, b=0.7, P=16), and in Fig. 12 when the parameters are (a=1, b=1, P=16).

The top of Fig. 11 shows the Doppler-delay scene at 3.274 seconds. We see about ten cars driving slowly away from the radar, presumably on the one-way alley. Their range-rates spread between 4 to 9 m/s and their ranges stretch from 50 to 250 m. The arrow points at the only prominent target that moves toward the radar $\left(r \approx 110\text{m},\ \dot{r} \approx -1\text{m/s}\right)$. We guess that it is target 1. The bottom of Fig. 11 displays the same scene 1.8 seconds later. Each car is now about 15m farther away. Target 1 remains at about the same range but is now moving away from the radar at a rate of $\dot{r} \approx +0.5\text{m/s}$. That pattern of slow back and forth motion of target 1, repeated itself several times.

We should point out that the range-rate outputs are blanked between $-0.44 \le \dot{r} \le 0.44\text{m/s}$, where clutter dominates. This means that target 1 was not visible when its radar return crossed the zero range-rate line. However it was clearly seen before (top) and after (bottom), at the very small radial velocities of –1m/s and +0.5m/s, respectivrly.

The lack of delay sidelobes is due to the fact that the phase-coded waveform had the property of perfect periodic correlation. The very low Doppler sidelobes were achieved by using a composite weight window, described in [10]. Some cars exhibit micro-Doppler returns, reflected from their wheels. Those should not be mistaken as Doppler sidelobes. The same two scenes were processed also with the binomial canceller parameters, namely (a=1, b=1). (Fig. 12), this time target 1 is much weaker on the top subplot, at $r \approx 110\text{m}$, $\dot{r} \approx -1\text{m/s}$, and barely seen on the bottom subplot, at $r \approx 110\text{m}$, $\dot{r} \approx +0.5\text{m/s}$. Apparently, the additional attenuation made a big difference.

VII. Conclusion

An application-specific optimization of the MTI filter/FFT combination was suggested and implemented by changing the tap parameters of a 3-pulse canceller and by increasing the delay between the taps from one PRI to many PRIs. The demonstrated combined Doppler response was designed to enhance slow targets. The penalties are lower blind velocities and smaller clutter attenuation. Both penalties are acceptable when the interest is in slow targets.

References

[1] L. Cartledge, and R. M. O'Donnel, "Description and performance evaluation of the moving target detector," Project Report ATC-69, MIT Lincoln Laboratory, 8 March 1977.

[2] D. C. Schleher, *MTI and Pulse Doppler Radar*, Boston: Artech, 1991.

[3] M. A. Richards, *Principles of Modern Radar – Basic Principles,* Raleigh, NC, Artech, 2010.

[4] J. Capon, "Optimum weighting functions for the detection of sampled signals in noise," *IEEE Trans. Information Theory,* vol. 10, no. 2, pp. 152-159, April 1962.

[5] J. K. Hsiao, "On the optimization of MTI clutter rejection," *IEEE Trans. Aerospace & Elect. Syst*., vol. 10, no. 5, pp.622-629, September 1974.

[6] A. I. Zverev, "Digital MTI radar filters," *IEEE Trans. Audio &v Electroacoustics*, vol. 16, no. 3, pp. 422-432, September 1968.

[7] W. W. Shrader, "MTI Radar," Ch. 17 in *Radar Handbook*, M. I. Skolnik, Ed., New York, McGraw Hill, 1970.

[8] F. J. Harris, "On the use of windows for harmonic analysis with the discrete Fourier transform," *IEEE Proc.*, vol. 68, no. 1, pp. 51-83, January 1978.

[9] K. M. M. Prabhu, *Window Functions and Their Applications in Signal Processing,* Boca Raton, FL, CRC Press, 2014.

[10] I. Cohen, and N. Levanon, "Weight windows – an improved approach," *2014 IEEE 28'th Conv. of Electrical & Electronics Eng. in Israel*, 3-5 December 2014. (http://ieeexplore.ieee.org/stamp/stamp.jsp?tp=&arnumber=705852)

Fig. 10. The scene from the radar roof-top location.

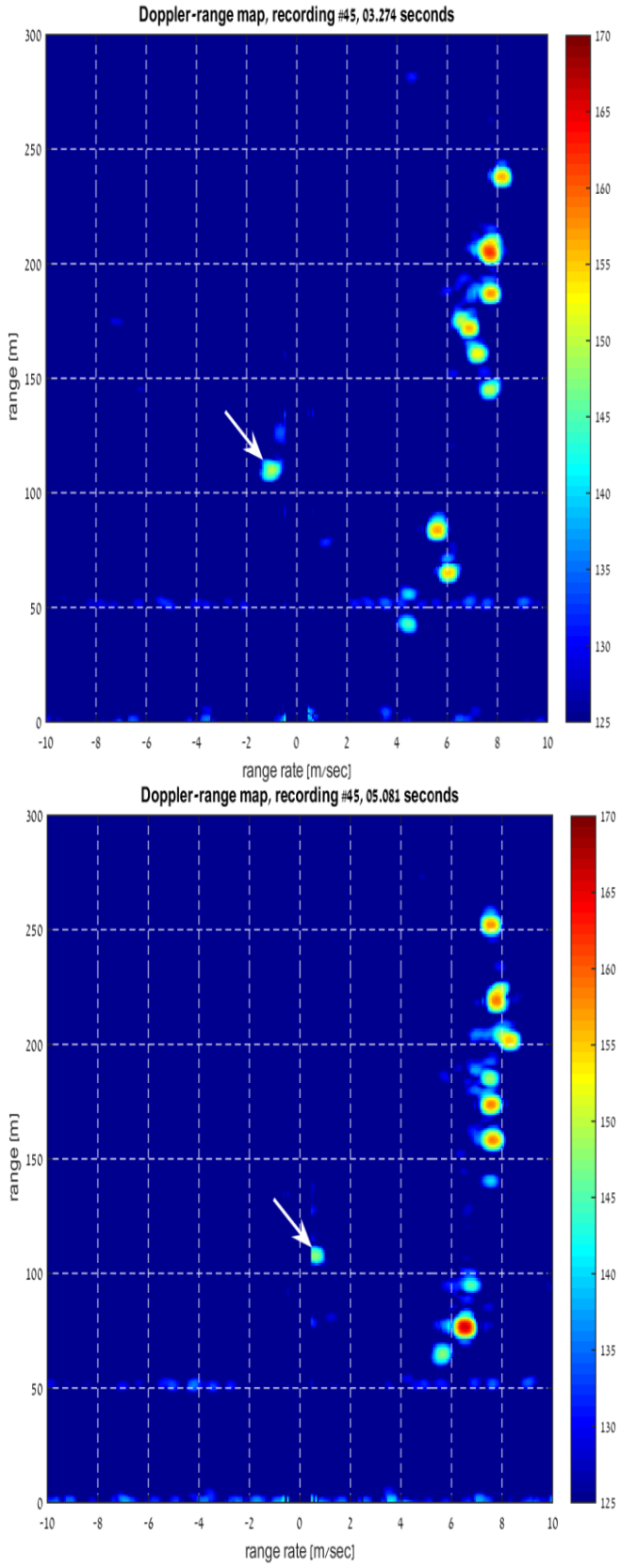

Fig. 11. (top) Delay-Doppler display at 3.274 seconds; (bottom) at 5.081 seconds. (a=0.7, b=0.7, P=16), Colorbar in dB.

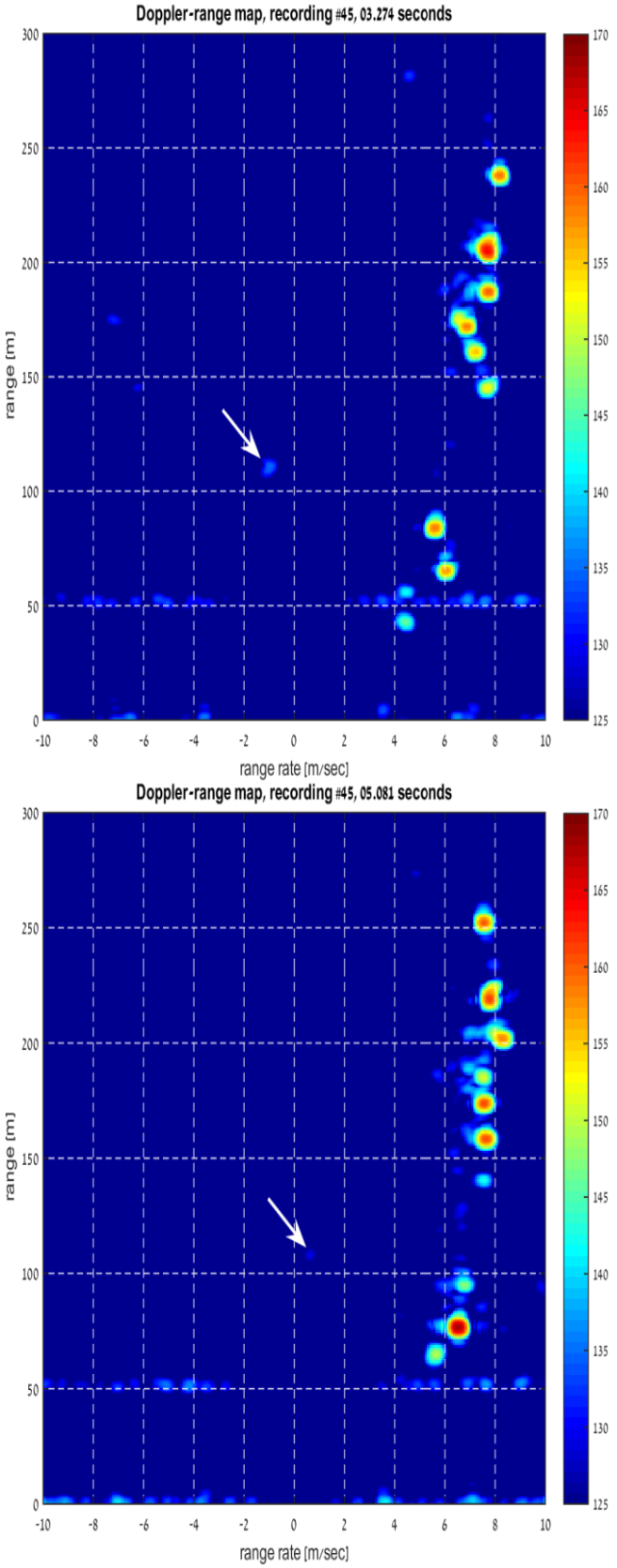

Fig. 12. (top) Delay-Doppler display at 3.274 seconds; (bottom) at 5.081 seconds. (a=1, b=1, P=16). Colorbar in dB.